Supplementary Information (SI) for Journal of Materials Chemistry C.

UV-C Emitting Phosphor of Pr^{3+}-Doped Fluoroborate Nano-Glass Composites for Disinfection and Fast Scintillator

Sikai Wang, [ab] **Ziyang Wu,** [ab] **Lei Sun,** [c] **Jinjun Ren,** [d] **Xiaoxin Zheng,** [*ab] **Jianzhong Zhang,** [ab] **Jing Ren,** [*ab]

[a] *Key Laboratory of In-fiber Integrated Optics of Ministry of Education, College of Physics and Optoelectronic Engineering, Harbin Engineering University, Harbin 150001, China*

[b] *Key Laboratory of Photonic Materials and Devices Physics for Oceanic Applications, Ministry of Industry and Information Technology of China, College of Physics and Optoelectronic Engineering, Harbin Engineering University, Harbin 150001, China*

[c] *Zhicheng College, Fuzhou University, Fuzhou 350002, China*

[d] *Key Laboratory of Materials for High Power Laser, Shanghai Institute of Optics and Fine Mechanics, Chinese Academy of Sciences, Shanghai 201800, China*

Corresponding authors: xxzheng@hrbeu.edu.cn, ren.jing@hrbeu.edu.cn

Thermal treatment condition optimization:

To determine the optimal annealing and thermal treatment temperatures, differential scanning calorimetry (DSC) tests were performed on the PG sample (**Fig. S1**). According to the DSC results, the heating process was initially carried out within the temperature range of 580-600°C for crystallization. Subsequently, thermal treatments were performed within this range to explore the impact on the material's properties.

As shown in **Fig. S2(b)**, X-ray diffraction (XRD) analysis revealed the various degrees of crystallization in the glass at different temperatures and durations. Specifically, the nanocrystals (NCs) precipitated within the glass matrix were identified as $Li(Al_7B_4O_{17})$. To achieve an optimal balance between high UV band transmittance and strong XEL intensity, a thermal treatment at 590°C for 10 hours was found to be the most favorable condition, as demonstrated in **Fig. S2(c)** and **S2(d)**.

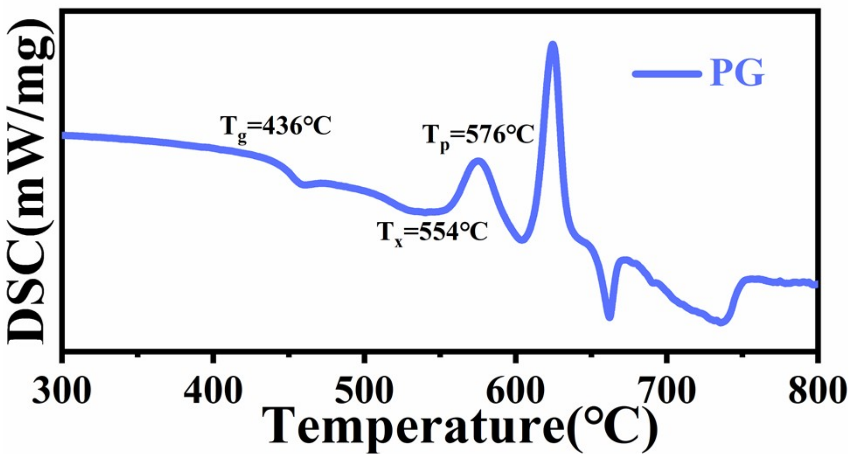

Fig. S1 DSC curve of the PG sample.

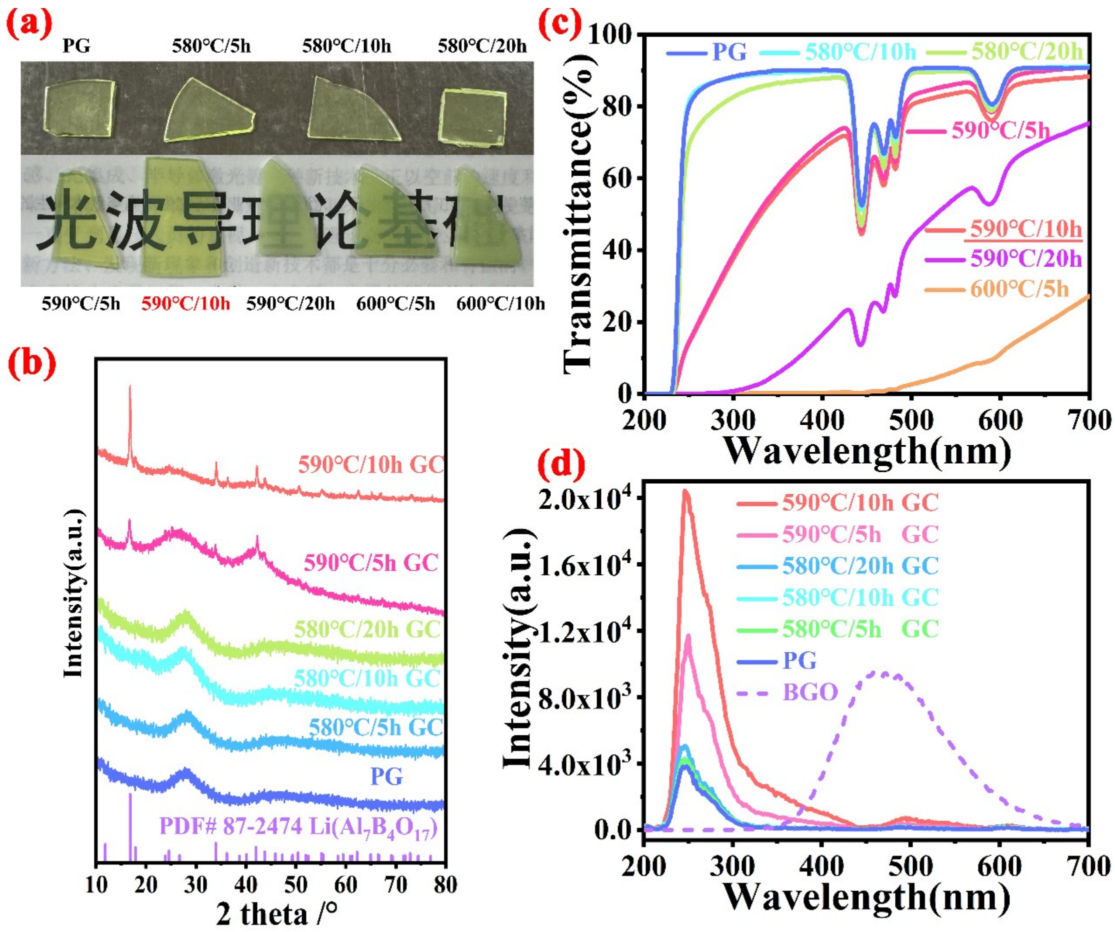

Fig. S2 (a) Photos of the Pr^{3+}-doped samples under various thermal treatment conditions; (b) XRD patterns of PG and GC samples; (c) Transmission spectra of PG and GC samples; (d) XEL spectra of PG and GC samples.

Composition optimization:

We have prepared a series of samples with the compositions of $40B_2O_3$ - $xBaF_2$ - (40-x) LiF - $20Al_2O_3$ (x = 0, 5, 10, 15, 20, 25, 30, 35, 40 in mol.%) abbreviated as x Ba-(40-x)Li. The optimization of Pr^{3+} ions doping concentration was also investigated in 10Ba-30Li system which mentioned in main text (Fig. S3 (b)).

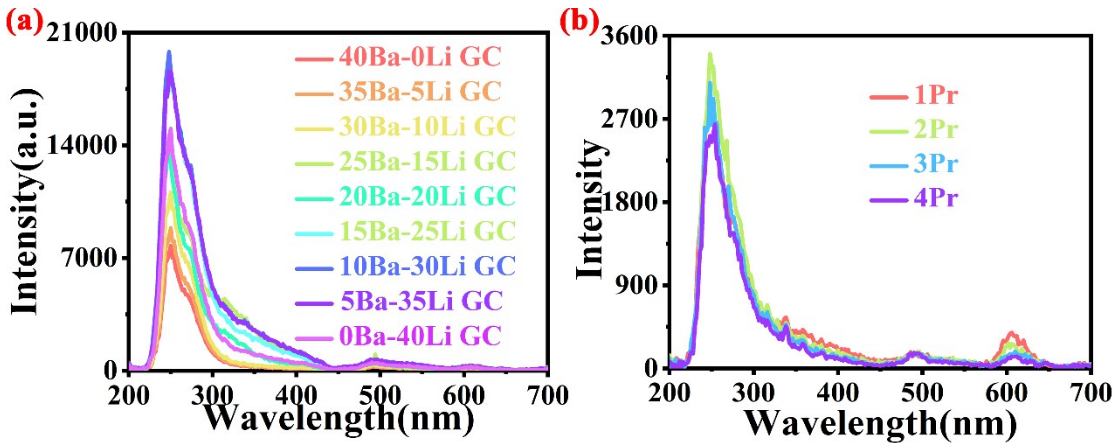

Fig. S3 (a) XEL spectra of Pr^{3+}-doped fluoroborate GC samples; (b) XEL spectra of different Pr^{3+} ions doping concentration in $40B_2O_3$ - $10BaF_2$ - 30LiF - $20Al_2O_3$ glass.

Table S1 Assignment of main Raman scattering bands of samples

Wavenumber (cm^{-1})	Raman assignments	Reference
550	Transverse motion of bridging oxygen within Al^{IV}-O-Al^{IV} linkages/loose diborate group	[1,2]
677	B-O-B stretching in metaborate rings	[3]
780	Al-O stretch vibrations of AlO_4 tetrahedral structural units with different numbers of non-bridging oxygen (NBO)/symmetric breathing vibration of six-membered rings with one or two $[BO_4]$/borate superstructures such as ditriborates, and penta-, tetra- or tri-borate species	[4–7]
840	Pyroborate vibrations	[8]
920	Vibration of orthoborate $[BO_3]$ structural units	[4,9,10]
1013	$[BO_4]^-$ units linked to borate groups containing NBO	[11]
1238	Trigonal boron groups, stretching of terminal B-O bonds in metaborate units, pyro-borate groups	[8]
1298	High frequency Raman bands to the B–O bonds linked to large borate groups	[10]
1406	Vibration of $[BO_3]$ triangle units	[12]
1505	Longitudinal B-O metaborate rings, $[BO_2O]^-$ triangles connected to other borate triangular units	[10]
1784	$Li(Al_7B_4O_{17})$ crystal phase	[13]

Table S2 The Judd-Ofelt intensity parameters (Ω_λ, $\times 10^{-20}$ cm^2) of glass system containing Pr^{3+} ions

Sample	Ω_2	Ω_4	Ω_6	References
Germanate	6.93	19.68	8.95	[14]
Silicate	5.40	3.88	7.41	[15]

Tellurite	3.84	7.64	5.90	[16]
Borate	1.33	6.81	8.62	[17]
Fluoroborate	0.98	4.67	4.96	[18]
Borovanadate	1.704	2.689	4.937	[19]
Phosphate	1.51	18.03	19.81	[20]
ZBLAN	2.44	4.41	5.52	[21]
PbB_4O_7 PG	5.917	4.77	21.35	[22]
PbB_4O_7 GC	2.476	4.638	20.727	[22]
CaF_2 PG	5.49	2.66	5.03	[23]
CaF_2 GC	2.10	2.88	2.01	[23]
SrF_2 PG	1.83	18.82	6.25	[24]
SrF_2 GC	0.18	3.83	1.24	[24]
PG	0.242	1.793	8.972	This work
GC	0.161	1.356	14.042	This work

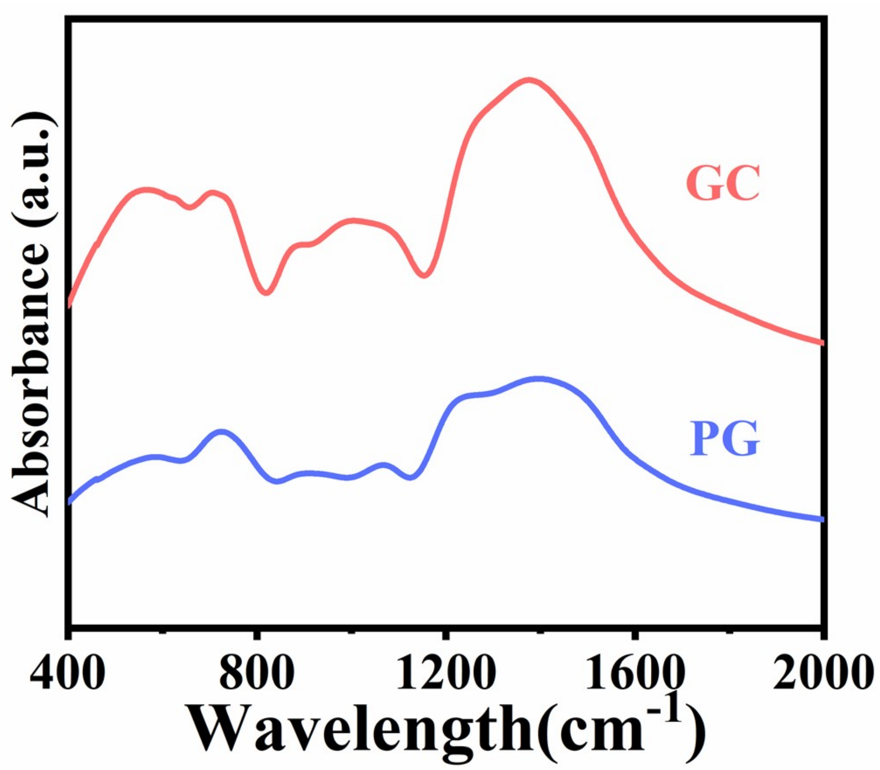

Fig. S4 FTIR spectra of PG and GC.

Table S3 Assignment of FT-IR spectrum distribution of samples

Wavenumber (cm^{-1})	FT-IR assignments	Ref.
560	Specific vibrations of Ba-O bonds	[25]
710	Stretching vibrations of Al-O bonds in AlO_6 groups; Bending vibrations of B-O-B; Vibration of $[BO_3]$ bending vibration; BO_3-O-BO_3 bond bending vibrations	[26–29]

883	Asymmetric stretching of B-O in $[BO_4]$	30
910	Stretching vibration of BO_4 units in various structural groups; Vibration of Al-O bonds in AlO_4 group	6,29
990	B-O-B bond stretching vibrations in $[BO_4]$	11,31
1066	B-O stretching vibrations of BO_4 units from tri, tetra, and pentaborate groups; Symmetric stretching of B-O in $[BO_4]$	29,32
1238	Asymmetric stretching vibrations of B-O bonds from orthoborate groups; B-O stretching vibrations of trigonal $[BO_3]$ units in meta-, pyro and ortho-borate groups	28,29,33
1366	Symmetric stretching vibrations of $[BO_3]$ groups; B-O bond stretching vibration of BO_3 of various borate rings	29,34
1480	Asymmetric stretching modes of borate triangles BO_3 units; $B-O^-$ bond stretching in BO_3	28,29

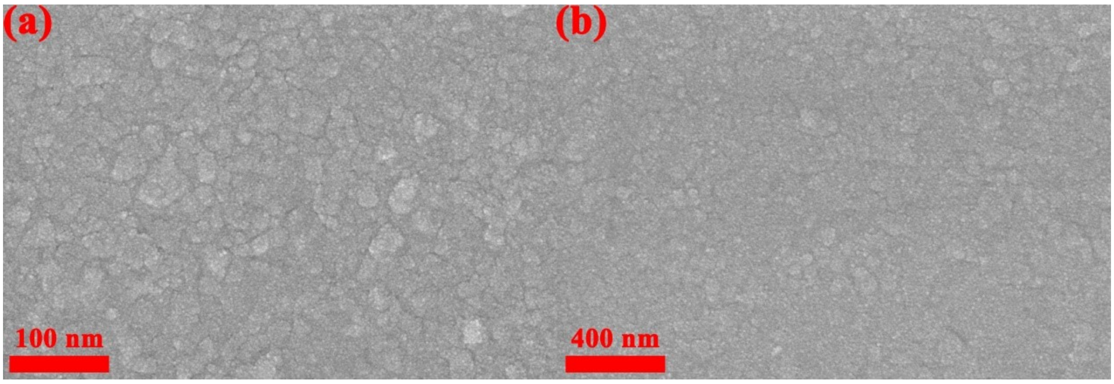

Fig. S5 SEM images of GC.

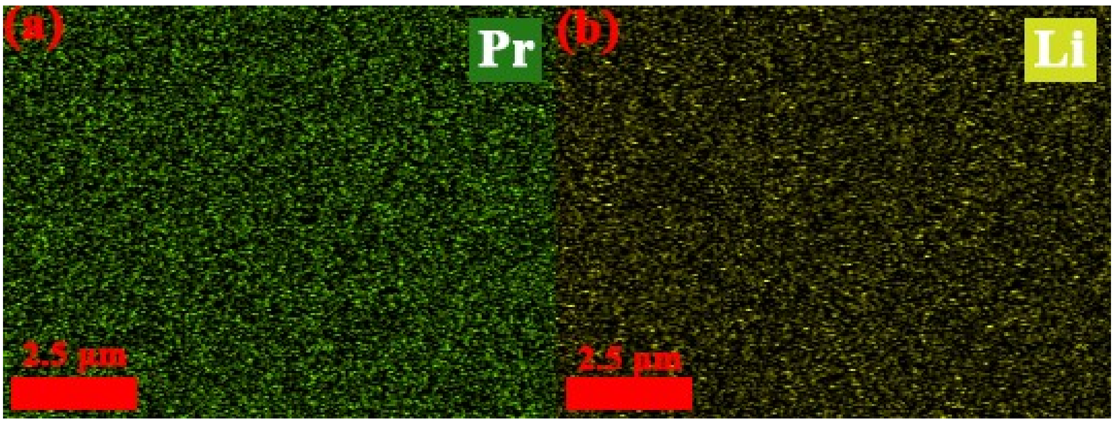

Fig. S6 Elemental mappings of (a) Pr, (b) Li, with the concentrations reflected by the brightness in color.

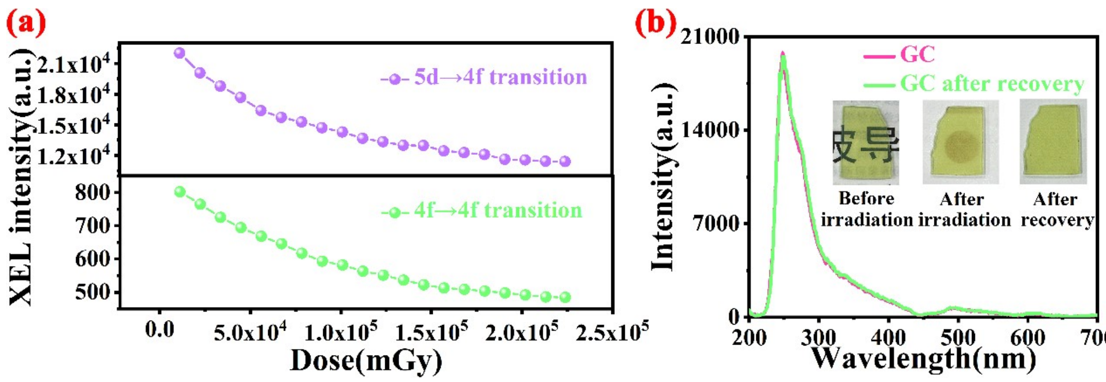

Fig. S7 (a)Various of XEL intensities of the 5d → 4f (250 nm) and 4f → 4f emissions (494 nm) in GC versus irradiation dose; (b) XEL spectra of GC and GC after thermal recovery; Inset: GC photos before and after X-ray irradiation; And GC photo after thermal recovery.

Table S4 Summary of cost of several luminescent materials.

Materials	Unit Price ($/cm^3)	Ref.
LYSO: Ce^{3+}	150	[35]
LuAG: Ce^{3+}	150	[35]
CsI: Tl	50	[36]
LSO: Ce^{3+}	40	[37]
BGO	9	[37]
ZBLAN glass: Pr^{3+}	5.1	[38]
Fluoroborate glass: Pr^{3+}	2.6	This work

Table S5 Parameters of fast scintillators.

Sample	Light Yield (Photons/MeV)	Decay time	Ref.
BaF_2	1,400	800 ps	[39–41]
LuAG: Pr^{3+}	19,000	20 ns	[42,43]
LuYAG: Pr^{3+}	33,000	20 ns	[44]
YAP: Pr^{3+}	12,000	10 ns	[45]
YAG: Ce^{3+}	28,000	90 ns	[46–48]
YAP: Ce^{3+}	17,000	26.7 ns	[49]
LuAG: Ce^{3+}	40,200	62.35 ns	[50]
LuYAP: Ce^{3+}	14,000	17 ns	[51]
GGAG: Ce^{3+}	50,000	90 ns	[52,53]

GYGAG: Ce^{3+}	50,000	-	[54]
GSO: Ce^{3+}	10,000	25 ns	[55]
Lu_2SiO_5: Ce^{3+}	30,000	42 ns	[56,57]
$LuBr_3$: Ce^{3+}	32,000	50 ns	[58]
$LuCl_3$: Ce^{3+}	13,000	4 µs	[58]
LuI_3: Ce^{3+}	42,000	35 ns	[59,60]
$LaCl_3$: Ce^{3+}	50,000	24 ns	[56,58]
$LaBr_3$: Ce^{3+}	78,000	15 ns	[61]
LaI_3: Ce^{3+}	95,000	24 ns	[56]
LGSO: Ce^{3+}	19,000	23 ns	[55]
LYSO: Ce^{3+}	30,000	30 ns	[62]
LSO: Ce^{3+}	20,000	28 ns	[55]
$CeBr_3$	68,000	17 ns	[63]
BGO	10000	300 ns	[64,65]
$KLaF_4$ GC: Ce^{3+}	17,000	53.6 ns	[66]
$Na_5Lu_{9-x}Gd_xF_{32}$ GC: Ce^{3+}	8,000	52.7 ns	[67]
Fluorosilicate GC: Pr^{3+}	5,832	23 ns (UV)	[68]
Fluoroborate GC: Pr^{3+}	**8,567**	**21.53 ns (UV)** **24.13 ns (γ-ray)**	**This work**

References

1 P. McMillan, B. Piriou and A. Navrotsky, *Geochim. Cosmochim. Acta*, 1982, **46**, 2021–2037.

2 W. L. Konijnendijk, Phd Thesis 1 (Research TU/e / Graduation TU/e), Technische Hogeschool Eindhoven, 1975.

3 C. N. Santos, D. De Sousa Meneses, P. Echegut, D. R. Neuville, A. C. Hernandes and A. Ibanez, *Appl. Phys. Lett.*, 2009, **94**, 151901.
4 W. L. Konijnendijk and J. M. Stevels, *J. Non-Cryst. Solids*, 1975, **18**, 307–331.
5 D. R. Neuville, G. S. Henderson, L. Cormier and D. Massiot, *Am. Mineral.*, 2010, **95**, 1580–1589.
6 E. I. Kamitsos and G. D. Chryssikos, *J. Mol. Struct.*, 1991, **247**, 1–16.
7 B. N. Meera and J. Ramakrishna, *J. Non-Cryst. Solids*, 1993, **159**, 1–21.
8 A. K. Yadav and P. Singh, *RSC Adv.*, 2015, **5**, 67583–67609.
9 D. Maniu, T. Iliescu, I. Ardelean, S. Cinta-Pinzaru, N. Tarcea and W. Kiefer, *J. Mol. Struct.*, 2003, **651–653**, 485–488.
10 E. I. Kamitsos, M. A. Karakassides and G. D. Chryssikos, *J. Phys. Chem.*, 1987, **91**, 1073–1079.
11 Q. Hu, T. Wang, Y. Chu, X. Wang, Y. Du, J. Ren, X. Yang, G. Yang, X. Kong and P. Wang, *J. Am. Ceram. Soc.*, 2019, **102**, 4562–4572.
12 T. Yano, N. Kunimine, S. Shibata and M. Yamane, *J. Non-Cryst. Solids*, 2003, **321**, 137–146.
13 P. S. Shirshnev, V. L. Ugolkov, Zh. G. Snezhnaia, D. I. Panov, E. V. Shirshneva-Vaschenko, S. N. Lipnitskaya, A. E. Romanov and V. E. Bougrov, *Rev. Adv. Mater. Sci.*, 2018, **57**, 116–120.
14 L. Żur, J. Janek, M. Sołtys, J. Pisarska and W. A. Pisarski, *J. Am. Ceram. Soc.*, 2016, **99**, 2009–2016.
15 A. L. Fanai, U. Khan and S. Rai, *J. Non-Cryst. Solids*, 2019, **503–504**, 89–93.
16 J. Hormadaly and R. Reisfeld, *J. Non-Cryst. Solids*, 1979, **30**, 337–348.
17 M. V. Sasi kumar, B. Rajeswara Reddy, S. Babu, A. Balakrishna and Y. C. Ratnakaram, *J. Taibah Univ. Sci.*, 2017, **11**, 593–604.
18 P. Babu and C. K. Jayasankar, *Phys. B*, 2001, **301**, 326–340.
19 M. El Okr, M. Farouk, M. El-Sherbiny, M. A. K. El-Fayoumi and M. G. Brik, *J. Alloys Compd.*, 2010, **490**, 184–189.
20 Ch. Basavapoornima, C. R. Kesavulu, T. Maheswari, W. Pecharapa, S. R. Depuru and C. K. Jayasankar, *J. Lumin.*, 2020, **228**, 117585.
21 R. S. Quimby, P. A. Tick, N. F. Borrelli and L. K. Cornelius, *J. Appl. Phys.*, 1998, **83**, 1649–1653.
22 T. Satyanarayana, M. G. Brik, N. Venkatramaiah, I. V. Kityk, K. J. Plucinski, V. Ravikumar and N. Veeraiah, *J. Am. Ceram. Soc.*, 2010, **93**, 2004–2011.
23 Q. J. Chen, W. J. Zhang, X. Y. Huang, G. P. Dong, M. Y. Peng and Q. Y. Zhang, *J. Alloys Compd.*, 2012, **513**, 139–144.
24 C. R. Kesavulu, C. S. D. Viswanath, S. Karki, P. Aryal, H. J. Kim and C. K. Jayasankar, *Ceram. Int.*, 2018, **44**, 1737–1743.
25 F. F. Bentley, L. D. Smithson and A. L. Rozek, *Infrared spectra and characteristic frequencies [equivalency symbol] 700-300 cm^{-1}*, Interscience, New York, 1968.
26 H. Fan, L. Hu, K. Yang and Y. Fang, *J. Non-Cryst. Solids*, 2010, **356**, 1814–1818.
27 C. Maalegoundla, K. C. Sekhar, A. Hameed, B. Srinivas and M. Shareefuddin, *J. Aust. Ceram. Soc.*, 2022, **58**, 1137–1146.
28 G. Padmaja and P. Kistaiah, *J. Phys. Chem. A*, 2009, **113**, 2397–2404.

29 J. D. M. Dias, G. H. A. Melo, T. A. Lodi, J. O. Carvalho, P. F. Façanha Filho, M. J. Barboza, A. Steimacher and F. Pedrochi, *J. Rare Earths*, 2016, **34**, 521–528.
30 M. Mączka, J. Hanuza, A. Pajączkowska, Y. Morioka and J. H. van der Maas, *J. Raman Spectrosc.*, 2004, **35**, 266–273.
31 B. Liu and Z. Zhu, *J. Non-Cryst. Solids*, 2023, **609**, 122265.
32 R. A. Kumar, M. Senthilkumar and R. Dhanasekaran, *Cryst. Res. Technol.*, 2008, **43**, 467–472.
33 H. Guo, Y. Wang, Y. Gong, H. Yin, Z. Mo, Y. Tang and L. Chi, *J. Alloys Compd.*, 2016, **686**, 635–640.
34 L. Jun, X. Shuping and G. Shiyang, *Spectrochim. Acta, Part A*, 1995, **51**, 519–532.
35 N. Tuccori, PhD Thesis, University of Sussex, 2023.
36 M. Kagaya, H. Katagiri, R. Enomoto, R. Hanafusa, M. Hosokawa, Y. Itoh, H. Muraishi, K. Nakayama, K. Satoh, T. Takeda, and others, *Nucl. Instrum. Methods Phys. Res., Sect. A*, 2015, **804**, 25–32.
37 F. Hueso-González, A. K. Biegun, P. Dendooven, W. Enghardt, F. Fiedler, C. Golnik, K. Heidel, T. Kormoll, J. Petzoldt, K. E. Römer, R. Schwengner, A. Wagner and G. Pausch, *J. Instrum.*, 2015, **10**, P09015.
38 H. Yang, Z. Dai, J. Li and Y. Tian, *J. Non-Cryst. Solids*, 2006, **352**, 5469–5474.
39 C. Van Eijk, J. Andriessen, P. Dorenbos, J. Jansons, N. Khaidukov, Z. Rachko and J. Valbis, 1993, pp. 161–166.
40 M. Laval, M. Moszyński, R. Allemand, E. Cormoreche, P. Guinet, R. Odru and J. Vacher, *Nucl. Instrum. Methods Phys. Res.*, 1983, **206**, 169–176.
41 R. Shendrik and E. Radzhabov, *IEEE Trans. Nucl. Sci.*, 2014, **61**, 406–410.
42 W. Drozdowski, P. Dorenbos, J. T. M. de Haas, R. Drozdowska, A. Owens, K. Kamada, K. Tsutsumi, Y. Usuki, T. Yanagida, and A. Yoshikawa, *IEEE Trans. Nucl. Sci.*, 2008, **55**, 2420–2424.
43 J. M. Herzog, D. Witkowski and D. A. Rothamer, *J. Lumin.*, 2021, **229**, 117665.
44 W. Drozdowski, K. Brylew, A. J. Wojtowicz, J. Kisielewski, M. Świrkowicz, T. Łukasiewicz, J. T. M. de Haas and P. Dorenbos, *Opt. Mater. Express*, 2014, **4**, 1207–1212.
45 C. W. E. van Eijk, P. Dorenbos, and R. Visser, *IEEE Trans. Nucl. Sci.*, 1994, **41**, 738–741.
46 P. Schauer and J. Bok, *Nucl. Instrum. Methods Phys. Res., Sect. B*, 2013, **308**, 68–73.
47 G. Zhao, X. Zeng, J. Xu, Y. Xu and Y. Zhou, *J. Cryst. Growth*, 2003, **253**, 290–296.
48 V. Bachmann, C. Ronda and A. Meijerink, *Chem. Mater.*, 2009, **21**, 2077–2084.
49 M. Moszyński, M. Kapusta, D. Wolski, W. Klamra and B. Cederwall, *Nucl. Instrum. Methods Phys. Res., Sect. A*, 1998, **404**, 157–165.
50 T. Wang, S. Hu, T. Ji, X. Zhu, G. Zeng, L. Huang, A. N. Yakovlev, J. Qiu, X. Xu and X. Yu, *Laser Photonics Rev.*, 2024, **18**, 2300892.
51 A. N. Belsky, E. Auffray, P. Lecoq, C. Dujardin, N. Garnier, H. Canibano, C. Pedrini, and A. G. Petrosyan, *IEEE Trans. Nucl. Sci.*, 2001, **48**, 1095–1100.
52 Y. Wu, J. Luo, M. Nikl and G. Ren, *APL Mater.*, 2014, **2**, 012101.

53 S. Yamamoto, J. Kataoka, K. Kamada and A. Yoshikawa, *Nucl. Instrum. Methods Phys. Res., Sect. A*, 2019, **919**, 125–133.
54 N. J. Cherepy, J. D. Kuntz, Z. M. Seeley, S. E. Fisher, O. B. Drury, B. W Sturm, T. A. Hurst, R. D. Sanner, J. J. Roberts, and S. A. Payne, 2010, **7805**, 78050I.
55 V. Jarý, E. Mihóková, J. A. Mareš, A. Beitlerová, D. Kurtsev, O. Sidletskiy and M. Nikl, *J. Phys. D: Appl. Phys.*, 2014, **47**, 365304.
56 K. W. Krämer, P. Dorenbos, H. U. Güdel and C. W. E. van Eijk, *J. Mater. Chem.*, 2006, **16**, 2773–2780.
57 C. M. Michail, G. P. Fountos, S. L. David, I. G. Valais, A. E. Toutountzis, N. E. Kalyvas, I. S. Kandarakis and G. S. Panayiotakis, *Meas. Sci. Technol.*, 2009, **20**, 104008.
58 O. Guillot-Noël, J. T. M. de Haas, P. Dorenbos, C. W. E. van Eijk, K. Krämer and H. U. Güdel, *J. Lumin.*, 1999, **85**, 21–35.
59 M. D. Birowosuto, P. Dorenbos, C. W. E. van Eijk, K. W. Krämer and H. U. Güdel, *J. Appl. Phys.*, 2006, **99**, 123520.
60 Z. Marton, V. V. Nagarkar, S. R. Miller, C. Brecher, H. B. Bhandari, P. Kenesei, S. K. Ross, J. D. Almer and B. Singh, *J. Phys.: Conf. Ser.*, 2014, **493**, 012017.
61 M. S. Alekhin, D. A. Biner, K. W. Krämer and P. Dorenbos, *J. Appl. Phys.*, 2013, **113**, 224904.
62 D. W. Cooke, K. J. McClellan, B. L. Bennett, J. M. Roper, M. T. Whittaker, R. E. Muenchausen and R. C. Sze, *J. Appl. Phys.*, 2000, **88**, 7360–7362.
63 W. M. Higgins, A. Churilov, E. van Loef, J. Glodo, M. Squillante and K. Shah, *J. Cryst. Growth*, 2008, **310**, 2085–2089.
64 M. J. Weber and R. R. Monchamp, *J. Appl. Phys.*, 1973, **44**, 5495–5499.
65 E. Sakai, *IEEE Trans. Nucl. Sci.*, 1987, **34**, 418–422.
66 B. Sun, Y. Xie, Y. Zhao, X. Li, J. Chen, Y. Song, L. Zhao, Z. Li, H. Zhao, J. Ren and J. Zhang, *J. Mater. Chem. C*, 2021, **9**, 17504–17510.
67 R. Wei, P. Dai, X. Tian, L. Ma, Q. Yu, F. Hu, L. Chen and H. Guo, *J. Eur. Ceram. Soc.*, 2024, **44**, 2418–2426.
68 S. Wang, C. Hua, L. Wang, C. Wang, L. Liu, J. Ren and J. Zhang, *Adv. Opt. Mater.*, 2024, **12**, 2302086.